The 2010 IEEE/RSJ International Conference on
Intelligent Robots and Systems
October 18-22, 2010, Taipei, Taiwan

On–line State and Parameter Estimation of an Under–actuated Underwater Vehicle using a Modified Dual Unscented Kalman Filter

George C. Karras Savvas G. Loizou Kostas J. Kyriakopoulos

Abstract— **This paper presents a novel modification of the Dual Unscented Kalman Filter (DUKF) for the on–line concurrent state and parameter estimation. The developed algorithm is successfully applied to an under-actuated underwater vehicle. Like in the case of conventional DUKF the proposed algorithm demonstrates quick convergence of the parameter vector. In addition, experimental results indicate an increased performance when the proposed methodology is utilized.**

The applicability and performance of the proposed algorithm is experimentally verified by combining the proposed DUKF with a non-linear controller on a modified Videoray ROV in a test tank. The on-line estimation of the vehicle states and dynamic parameters is achieved by fusing data from a Laser Vision System (LVS) and an Inertial Measurement Unit (IMU).

I. INTRODUCTION

Underwater vehicles usually operate in circumstances demanding dexterous operations and delicate motions, such as the inspection of ship hulls, propulsion system or other underwater structures. In most of these cases closed loop control schemes can provide more efficient and accurate results than a typical open-loop teleoperation scenario. In the later case, the operator must perform accurate manoeuvres, while dealing with strong currents, waves and also compensate for the ROV's tether. Additionally, teleoperation becomes even more difficult, considering that most of the underwater vehicles (especially some small class ROV's) suffer from kinematic constraints due to under-actuation. Thus, a fully or semi-autonomous steering control scheme is most likely the appropriate solution for complex underwater inspection tasks.

In order to design a robust control scheme, a suitable dynamic model of the vehicle must first be considered and identified. The system's equations may vary depending of the vehicle configuration, actuation capabilities, operating speed and planes of symmetry [1]. In [2], a comparison between two methods for the off-line identification of an unmanned underwater vehicle (UUV) has been presented. The first is based on the minimization of the acceleration prediction error, while the other on the minimization of the velocity prediction error. In [3] a Least-Squares (LS) based identification of a lumped parameter model of open-frame UUV is presented, while the effects of propeller-hull and propeller-propeller interactions are considered. Moreover, in [4] the dynamic model of an under-actuated underwater vehicle is identified using an off-line LS technique, considering the presence of slowly varying unknown disturbances.

Most of the above mentioned off-line techniques can provide sufficiently accurate results, but they usually require a large amount of input-output data, expensive sensor suites and dedicated experimental setups. Generally, off-line identification is a time consuming process that takes place in-situ and if the configuration of the vehicle changes (i.e addition or removal of sensors or tools) the procedure must be repeated.

In [5] an on-line adaptive technique for the identification of finite dimensional dynamical models of dynamically positioned underwater robotic vehicles is described. The methodology was directly compared to the conventional off-line LS technique. Also, the use of neural networks in the identification of models for underwater vehicles is discussed in [6]. In all of these cases the complete state vector of the vehicle is assumed to be known or directly measured from dedicated sensors. Nevertheless, small underwater vehicles, usually don't carry large amount of sensors for payload and capacity reasons. The on–board camera and the IMU stand out as the most popular sensor suite for a small vehicle. So, estimation of non measurable states is an a priori requirement for an accurate parameter estimation process.

Efficient methods for on–line state and parameter estimation are based on the augmentation of the well known UKF algorithm for state estimation [7]. A description of the UKF applicability for the state and parameter estimation of non–linear systems as well as an analytical justification of the superiority of the UKF over the EKF parameter estimation techniques can be found in [8]. The description of the two most popular techniques, joint and dual UKF, can be found in [9].

In this paper, a Modified Dual Unscented Kalman (MDUKF) filter algorithm for the state and parameter estimation of an underwater vehicle is presented. The non–linear measurement model of the parameter estimation filter is rearranged in the form $\tau = \mathbf{Y}\pi$ used in most off-line LS techniques, where τ is the input vector, $\mathbf{Y}$ a matrix containing non–linear expressions of the vehicle's states and π the parameter vector to be identified. It is experimentally verified that the proposed methodology demonstrates quick convergence of the parameter vector while yielding minimized errors between the actual and predicted inputs. This latter property has not been demonstrated by the previous versions of the Dual UKF; however in this work our experimental results clearly indicate that with the proposed approach we can achieve minimization of the error between

G.C. Karras and K.J. Kyriakopoulos are with the Control Systems Lab, School of Mechanical Engineering, National Technical University of Athens, 9 Heroon Polytechniou Str., Zografou, Athens karrasg,kkyria@mail.ntua.gr

S.G. Loizou is with the School of Mechanical Engineering, Frederick University, Cyprus s.loizou@frederick.ac.cy

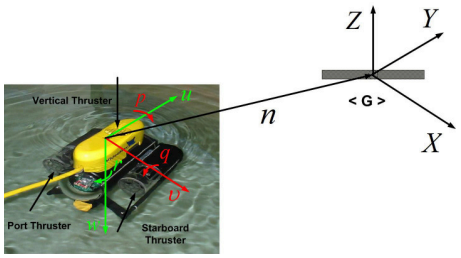

Fig. 1. Under-actuated ROV. Red color indicates under-actuated DOF, while green color indicates fully actuated DOFs.

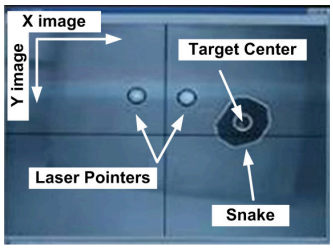

Fig. 2. Active Contours application

the actual and the predicted inputs. Since good initial estimates of the parameters play an important role in the eventual convergence of the filter our strategy to obtain good quality initial estimates of some of the decoupled parameters was to initially excite separately each (actuated) degree of freedom. Using this set of parameters as an initial estimate to the modified DUKF, a (non-linear) closed loop control scheme developed by the authors in [10], that is designed for inspection tasks is applied to the ROV. The experimental results indicate that the modified DUKF achieves a fine tuning of the parameters vector and a better description of the vehicle's dynamics is the outcome. On-line estimation of the vehicle states and dynamic parameters is achieved by fusing data from a Laser Vision System (LVS) and an Inertial Measurement Unit (IMU).

The rest of this paper is organized as follows: Section II gives an overview of the robot's kinematic and dynamic equations. Section III describes the on–line state and parameter estimation using the Modified Dual UKF approach. Section IV briefly describes the control scheme imposed for the fine tuning of the parameter vector. Section V illustrates the efficiency of our approach through an experimental procedure. Eventually, Section VI concludes the paper.

II. Preliminaries

We consider an underwater vehicle as a 6 DOF free body with position and Euler angle vector $\mathbf{n} = [x\ y\ z\ \phi\ \theta\ \psi]^T$. The body velocities vector is defined as $\mathbf{v} = [u\ v\ w\ p\ q\ r]^T$ where the components have been named according to SNAME as surge, sway, heave, roll, pitch and yaw respectively (Fig.1). The forces and moments vector acting on the body-fixed frame is defined as $\tau = [X\ Y\ Z\ K\ M\ N]^T$.

The vehicle used in this work is a 3 DOF VideoRay Pro ROV. It is equipped with three thrusters, which are effective only in surge, heave and yaw motion (Fig.1), while the vehicle is under-actuated along the sway axis. Roll and pitch motions are also without actuation but will not be dealt with in this work as they are considered to be negligible due to the passive stability properties of the vehicle. Hence the angles ϕ, θ and angular velocities p and q are assumed to be zero. The ROV is symmetric about the y - z plane and close to symmetric about the x - z plane. Due to the above assumptions and considering that the vehicle is operating at relative low speeds, the kinematic and dynamic model of the vehicle is given by the equations below:

$$\dot{\check{\mathbf{n}}} = \check{\mathbf{J}}(\psi)\,\check{\mathbf{v}} \tag{1}$$

$$\begin{aligned} m_{11}\dot{u} &= -m_{22}vr + X_u u + X_{u|u|}u\,|u| + X \\ m_{22}\dot{v} &= m_{11}ur + Y_v v + Y_{v|v|}v\,|v| \\ m_{33}\dot{w} &= Z_w w + Z_{w|w|}w\,|w| + Z \\ J\dot{r} &= N_r r + N_{r|r|}r\,|r| + N \end{aligned} \tag{2}$$

where: $\check{\mathbf{n}} = [x\ y\ z\ \psi]^T$, $\check{\mathbf{v}} = [u\ v\ w\ r]^T$, m_{ii} is the ii'th entry of the vehicle's inertia matrix M, J is vehicle's moment of inertia about z axis, $X_k, X_{k\|k\|}$, $Y_k, Y_{k\|k\|}$, $Z_k, Z_{k\|k\|}$, $N_k, N_{k\|k\|}$ where $k \in \{u, v, w, r\}$ are the linear and quadratic hydrodynamic coefficients in the surge, sway, heave and yaw respectively, while $\mathbf{J}(\mathbf{n})$ is the Jacobian matrix transforming the velocities from the body-fixed to earth-fixed frame.

III. On–line State and Parameter Estimation – Modified Dual UKF Approach

This section outlines the on–line state and parameter estimation process fusing data from the LVS and the IMU using a Dual UKF. In this fusion approach, two parallel filters are implemented in a closed–loop form, one for the state and another for the parameter estimation process. The state filter calculates an optimal estimation of the vehicle's state vector using the parameter vector at given time k. Then the state vector is served as input to the parameter filter where a new estimation of the vehicle's parameter vector is calculated. The new parameter vector is then served as input to the state estimation filter and the process continuous iteratively.

A. State Estimation

As mentioned before the complete state vector of the vehicle is estimated by fusing data from the LVS and an IMU using an UKF. The LVS consists of a CCD camera and two laser pointers which are parallel to the camera axis. The LVS calculates the pose vector of the vehicle with respect to the center of a target which lays on the image plane. The target center and borderline are tracked using the Active Contours (Snakes) computer vision algorithm [11], which is implemented in the system software. Note that the center of the Snake in the image space (u_{tc}, v_{tc}) coincides with the center of the target (see Fig. 2). The sensor model for the LVS is of the form:

$$\begin{bmatrix} u_{tc} \\ v_{tc} \\ L_1 \\ L_2 \end{bmatrix} = \mathbf{h}^{\alpha}(\check{\mathbf{n}}, \mathbf{w}^{\alpha}) \tag{3}$$

where L_1, L_2 are the ranges of each laser pointer from the surface the target is located and $\mathbf{w}^{\alpha}$ is zero mean white noise with covariance matrix $\mathbf{R}^{\alpha}$. The LVS is successfully used in previous works [12], [13]. The analytical expression of Eq. (3) and a more detailed description of the LVS can be found in [12].

The IMU used in this system (XSENS-MTi) provides 3D linear accelerations, 3D rate of turn and 3D orientation (Euler angles). The IMU weights only 50 gr and it is placed at the mass center of the vehicle aligned with its axes. The sensor model for the IMU that is implemented is of the form:

$$\begin{bmatrix} \hat{\psi} \\ \hat{r} \\ \hat{a_x} \\ \hat{a_y} \\ \hat{a_z} \end{bmatrix} = \mathbf{h}^{\beta} \left(\begin{bmatrix} \psi \\ r \\ a_x \\ a_y \\ a_z \end{bmatrix}, \mathbf{w}^{\beta} \right) \tag{4}$$

where $\mathbf{w}^{\beta}$ is a zero mean white noise with covariance matrix $\mathbf{R}^{\beta}$.

The equations describing the motion of the vehicle, as well as the equations describing the sensors are nonlinear. We choose to implement the Unscented Kalman Filter, which is a consistent estimator in order to calculate in real time the complete state vector of the vehicle:

$$\mathbf{p} = \begin{bmatrix} \breve{\mathbf{n}}^T & \breve{\mathbf{v}}^T & \dot{\breve{\mathbf{v}}}^{\mathbf{T}} \end{bmatrix}^T$$

Note that the measurements from the IMU and LVS sensor arrive at different rates and especially for the LVS those rates vary. In order to take into consideration the varying rate of the LVS sensor we need to appropriately shape our UKF fusion strategy. A multi-rate UKF was succesfully reported in [14]. Our approach is similar but we relax the assumption of constant rate measurement to produce an asynchronous fusion strategy. The system model that we implement is (1, 2), augmented with a 4-dimensional model for the accelerations to produce a 12-dimensional system model that is omitted in this paper for space considerations. The system model can be written as:

$$\dot{\mathbf{p}}(t) = \mathbf{f}(\mathbf{p}(t), \mathbf{U}(t)) + \mathbf{w}^{m}(t)$$

where $\mathbf{U}(t)$ is the input vector and $\mathbf{w}^{m}(t) \sim N(0, \mathbf{Q})$ is the process noise assumed to be zero mean white.

For the measurement model we have three different equations: the IMU measurement model (Eq. (4)), the LVS measurement model (Eq. (3)) and the IMU-LVS measurement model that is the augmentation of the two models, i.e.

$$\hat{\mathbf{y}} = \begin{bmatrix} \mathbf{h}^{\alpha}(\breve{\mathbf{n}}, \mathbf{w}^{\alpha}) \\ \mathbf{h}^{\beta}(\breve{\mathbf{n}}, \mathbf{w}^{\beta}) \end{bmatrix} \tag{5}$$

So at each iteration the fusion process actually uses only the sigma points corresponding to the sensor considered (i.e. the one that has produced the output at the current time instant) and the corresponding estimated output equation (i.e Eq. (3) if only an LVS measurement was received, Eq. (4) if only an IMU measurement was received, or Eq. (5) if an LVS and an IMU measurement were received concurrently). Moreover, the algorithm uses the corrector equations with only the subset of the outputs dictated by the sensor to obtain the state estimation (see also [7],[14]). The estimation can be produced at the time instant it is needed by propagating the model up to that time instant.

B. Parameter Estimation - The Modified Approach

The dynamic parameter vector is calculated using an UKF for on line parameter estimation. The parameter filter is executed at each time instant k, immediately after the state filter completes at the same time instant. The non–linear model of the parameter estimation filter is rearranged in the form $\tau = \mathbf{Y}\pi$, where τ is the input vector, $\mathbf{Y}$ a matrix containing non–linear expressions of the vehicle's states and π the parameter vector to be identified. Thus, the expected measurement matrix is of the form $\mathbf{Y} = \tau\,\pi^{\dagger}$, where $\pi^{\dagger} = \left(\pi^{\mathrm{T}}\pi\right)^{-1}\pi^{\mathrm{T}}$ is the Moore–Penrose pseudo–inverse matrix of π considering that columns of π are linearly independent. The equations are formulated as follows:

1) The filter is initialized with the predicted mean and covariance of the dynamic parameters:
$$\hat{\pi}_0 = E[\pi_{\mathbf{0}}]$$
$$\mathbf{P}_{\pi_{\mathbf{0}}} = E\left[(\pi_0 - \hat{\pi}_{\mathbf{0}})(\pi_0 - \hat{\pi}_{\mathbf{0}})^T\right]$$
2) The time update of the parameter vector and covariance is performed using:
$$\hat{\pi}_k^- = \hat{\pi}_{k-1}$$
$$\mathbf{P}_{\pi_{\mathbf{k}}}^- = \mathbf{P}_{\pi_{\mathbf{k-1}}} + \mathbf{Q}_{\pi_{\mathbf{k}}}$$
where $\mathbf{Q}_{\pi_{\mathbf{k}}}$ is the system process noise of the time update and is defined as in [8].
3) The sigma points are calculated from the a priori mean and covariance of the parameters using:
$$\mathbf{\Pi}_{k|k-1} = \begin{bmatrix} \hat{\pi}_k^-, & \hat{\pi}_k^- + \gamma_p\sqrt{\mathbf{P}_{\pi_{\mathbf{k}}}^-}, & \hat{\pi}_k^- - \gamma_p\sqrt{\mathbf{P}_{\pi_{\mathbf{k}}}^-} \end{bmatrix}$$
where $\gamma_p = \sqrt{n_p + \lambda}$, n_p the number of parameters and λ as defined in the state filter ([9]).
4) The expected measurement matrix $\mathbf{Y}_{i,k|k-1}$ for each row of $\mathbf{\Pi}_{k|k-1}$, is determined using the linear measurement model as follows:
$$\mathbf{Y}_{i,k|k-1} = \tau_{\mathbf{k}}\,\mathbf{\Pi}_{i,k|k-1}^{\dagger}$$
where $\mathbf{\Pi}_{i,k|k-1}^{\dagger}$ the pseudo–inverse of the $i-th$ row of matrix $\mathbf{\Pi}_{k|k-1}$. It is obvious that $\mathbf{Y}_{i,k|k-1}$ is a matrix filled with predicted measurements and zero elements, as imposed by the expression of $\mathbf{Y}$. In order to proceed to the next filter steps, we form the vector $\mathbf{b_{i,k|k-1}}$ containing only the non–zero elements of $\mathbf{Y}_{i,k|k-1}$.
5) The mean measurement $\hat{\mathbf{d}}_k$ and the measurement covariance $\mathbf{P}_{\mathbf{d_k d_k}}$, are calculated based on the statistics of the expected measurements:
$$\hat{\mathbf{d}}_k = \sum_{i=0}^{2n_p} w_i^{(m)}\mathbf{b_{i,k|k-1}}$$
$$\mathbf{P}_{\mathbf{d_k d_k}} = \sum_{i=0}^{2n_p} w_i^{(c)}\left(\mathbf{b_{i,k|k-1}} - \hat{\mathbf{d}}_k\right)\left(\mathbf{b_{i,k|k-1}} - \hat{\mathbf{d}}_k\right)^T + \mathbf{R}_{\pi_{\mathbf{k}}}$$

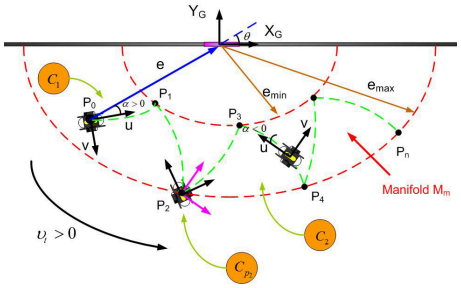

Fig. 3. Closed loop controller: Imposed trajectory to the ROV. Target should always remain within the field of view [10]

where $\mathbf{R}_{\pi_\mathbf{k}}$ the measurement noise covariance matrix for the parameter filter and $w_i^{(m)}$, $w_i^{(c)}$ as defined in the UKF state filter ([9]).

6) The cross-correlation covariance $\mathbf{P}_{\pi_\mathbf{k}\mathbf{d_k}}$, is calculated using:

$$\mathbf{P}_{\pi_\mathbf{k}\mathbf{d_k}} = \sum_{i=0}^{2n_p} w_i^{(c)} \left(\mathbf{\Pi}_{i,k|k-1} - \hat{\pi}_k^-\right) \left(\mathbf{b_{i,k|k-1}} - \hat{\mathbf{d}}_k\right)^T$$

7) The Kalman gain matrix is approximated from the cross-correlation and measurement covariances using:

$$\mathbf{K}_{\pi_\mathbf{k}} = \mathbf{P}_{\pi_\mathbf{k}\mathbf{d_k}} \mathbf{P}^{-1}_{\mathbf{d_k}\mathbf{d_k}}$$

8) The measurement update equations are:

$$\hat{\pi}_k^+ = \hat{\pi}_k^- + \mathbf{K}_{\pi_\mathbf{k}} \left(\mathbf{d}_k - \hat{\mathbf{d}}_k\right)$$
$$\mathbf{P}^+_{\pi_\mathbf{k}} = \mathbf{P}^-_{\pi_\mathbf{k}} - \mathbf{K}_{\pi_\mathbf{k}} \mathbf{P}_{\mathbf{d_k}\mathbf{d_k}} \mathbf{K}^\mathbf{T}_{\pi_\mathbf{k}}$$

where $\mathbf{d}_k$ the real measurement vector, which elements are produced from last estimations of the state filter.

IV. Closed–loop Control Scheme

As mentioned before the system is initially excited separately at each actuated DOF and a parameter vector is estimated using the DUKF. Then a fine tuning of the parameter vector is accomplished by exciting the actuators of the vehicle simultaneously using a closed loop control scheme which was designed for inspection tasks [10]. The controller is stripped–down in two parts. The first part is responsible for steering the vehicle in planar motions and imposes a sawtooth–like trajectory around a target of interest while guarantees the target will always remain inside the camera's field of view. The second part is responsible for the stabilization of the vehicle along the vertical (z) axis and it is accomplished by feed-forwarding the dynamics along z axis and a simple PD position controller. The planar trajectory imposed by the controller is denoted in Fig.3. More information about the closed–loop control scheme can be found in [10].

V. Experiments

In order to assess the overall efficiency of the system, two experimental sessions were carried out, one using open–loop sinusoidal inputs and another using the closed–loop control scheme described in IV. The experiments took place inside a water tank using a small underwater vehicle. The ROV used is a 3-DOF VideoRay PRO (VideoRay LLC, Fig.1), equipped with three thrusters, a control unit, and a CCD camera. The camera signal is acquired by a framegrabber (Imagenation PXC200). The LVS provides data asynchronously in the range of $10 - 17Hz$. The laser pointers are equipped with Sony diodes, with 635 nm wavelength. The IMU is an XSENS MT-i and delivers data at $512Hz$. An external position sensor (Polhemus, Isotrak), was used as the truth reference for the evaluation of the State Filter.

A. Experimental Results

In the first session the vehicle is separately excited at each actuated degree of freedom (Surge, Yaw, Heave) using open–loop sinusoidal inputs. The parameters are estimated using the Modified UKF approach. The evolution and eventual convergence of the parameters are depicted in Fig.4, Fig.5, Fig.6 for the actuated DOFs of Surge, Yaw and Heave respectively. The results of the estimated dynamic parameters using the Modified DUKF approach, are compared to the results provided by the 'classic' implementation of DUKF (see [8], [9]). The metric used for this comparison was coefficient of determination R^2 between the predicted and actual inputs for each case. The superiority of the Modified DUKF presented in this paper is shown in Fig.7, Fig.8 for Surge and Yaw. It should be mentioned that in our experiments, the 'classic' DUKF failed in the convergence of the parameters related to the Yaw DOF, thus no metric was available. The performance of the Modified and the 'classic' approach were similar in the Heave DOF as shown in Fig.9.

In the second session the vehicle is simultaneously excited at all degrees of freedom using the closed–loop control scheme described in IV. The parameter filter is initialized using the parameters calculated from the open–loop session. As can be seen from the experimental results of the second session (Fig.10 up to Fig.18) a fine tuning of the parameter vector is accomplished and additionally an approximation of the parameters related to the under–actuated DOF is accomplished. We present for the second session only the results of the Modified approach. First let us discuss the results of the state filter: In Fig.10 the estimation of the planar motion of the vehicle is shown in comparison to an external position sensor (truth reference). The estimation of the velocities in Surge and Sway is shown in Fig.11, Fig.12 respectively. No external velocity sensor was available, thus a direct comparison was not possible. Due to space reasons we omit the figures describing the estimation of the rest of the states. Instead we use as metric the trace of covariance matrix $\mathbf{P}_{\mathbf{p}_k}$ (Fig.13), in order to demonstrate the overall accuracy and convergence of the state filter. As can be seen, the trace gradually converges close to zero.

Regarding the performance of the modified parameter filter during the closed–loop control of the vehicle, the convergence of the parameters is shown in Fig.14, Fig.15, Fig.16, for Surge, Sway and Yaw DOFs respectively. The vehicle was kept at constant depth during the experiment,

so no results are presented for Heave. A comparison of the predicted and real (i.e. commanded) inputs is depicted in Fig.17, Fig.18, as well as, the values of R^2, which also prove the efficiency of the proposed methodology in closed–loop control.

VI. Conclusions

In this paper a novel modification of the Dual Unscented Kalman Filter (DUKF) for the on–line concurrent state and parameter estimation of an under-actuated underwater vehicle is presented. The main contribution is based on the rearrangement of the non–linear measurement model of the parameter estimation filter in the form $\tau = \mathbf{Y}\pi$. Like in the case of conventional DUKF the proposed algorithm demonstrates quick convergence of the parameter vector, while experimental results indicate an increased performance of the proposed methodology in terms of the accuracy of the parameter estimator part of the filter which in turn causes the state filter to yield improved estimations. The applicability and performance of the proposed algorithm is experimentally verified both in open and closed–loop excitations of the vehicle's thrusters.

References

[1] T. Fossen, "Guidance and control of ocean vehicles," *Wiley, New York*, 1994.

[2] P. Ridao, A. Tiano, A. El-Fakdi, M. Carreras, and A. Zirilli, "On the identification of non-linear models of unmanned underwater vehicles," *Control Engineering Practice 12*, pp. 1483–1499, 2004.

[3] M. Caccia, G. Indiveri, and G. Veruggio, "Modeling and identification of open frame variable configuration unmanned underwater vehicles," *IEEE Journal of Oceanic Engineering*, pp. 227–240, 2000.

[4] D. Panagou, G. Karras, and K. Kyriakopoulos, "Towards the stabilization of an underactuated underwater vehicle in the presence of unknown disturbances," *MTS/IEEE OCEANS*, 2008.

[5] D. Smallwood and L. Whitcomb, "Adaptive identification of dynamically positioned underwater robotic vehicles," *IEEE Transcactions on Control Systems Technology*, pp. 505–515, 2003.

[6] P. van de Ven, T. Johansen, A. Sorensen, C. Flanagan, and D. Toal, "Neural network augmented identification of underwater vehicle models," *Control Engineering Practice 15*, pp. 715–725, 2007.

[7] S. Julier and J. Uhlmann, "A new extension of the kalman filter to nonlinear systems," *Proc.of the Int. Symp. Aerospace/Defense Sensing, Simul. and Controls*, 1997.

[8] R. V. der Merwe and E. Wan, "The square-root unscented kalman filter for state and parameter-estimation," *IEEE International Conference on Acoustics, Speech, and Signal Processing*, pp. 3461–3464, 2001.

[9] M. VanDyke, J. Schwartz, and C. Hall, "Unscented kalman filtering for spacecraft attitude state and parameter estimation," *Advances in the Astronautical Sciences*, pp. 217–228, 2004.

[10] G. Karras, S. Loizou, and K. Kyriakopoulos, "A visual-servoing scheme for semi-autonomous operation of an underwater robotic vehicle using an imu and a laser vision system," *IEEE International Conference on Robotics and Automation*, 2010.

[11] M. Kass, A. Witkin, and D. Terzopoulos, "Snakes: Active contour models," *International Journal of Computer Vision*, pp. 321–331, 1987.

[12] G. Karras, D. Panagou, and K. Kyriakopoulos, "Target-referenced localization of an underwater vehicle using a laser-based vision system," *MTS/IEEE OCEANS*, 2006.

[13] G. Karras and K. Kyriakopoulos, "Visual servo control of an underwater vehicle using a laser vision system," *Proc. of IEEE/RSJ Intelligent Robots and Systems*, pp. 4116–4122, 2008.

[14] L. Armesto, S. Chroust, M. Vincze, and J. Tornero, "Multi-rate fusion with vision and inertial sensors," *Proc. of IEEE International Conference on Robotics and Automation*, pp. 193–199, 2004.

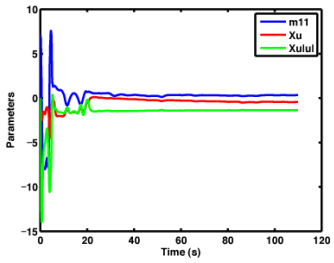

Fig. 4. Parameter Estimation in Surge: Open Loop Excitation

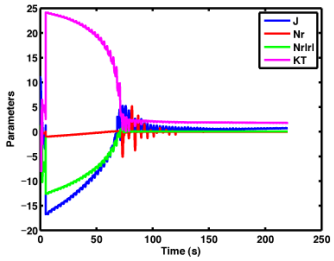

Fig. 5. Parameter Estimation in Yaw: Open Loop Excitation

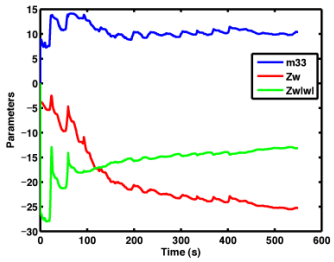

Fig. 6. Parameter Estimation in Heave: Open Loop Excitation

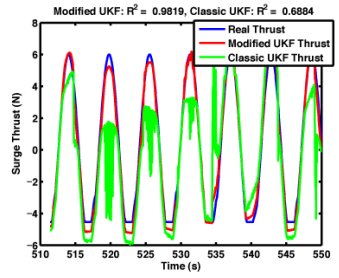

Fig. 7. Real vs Estimated Thrust in Surge: Open Loop Excitation

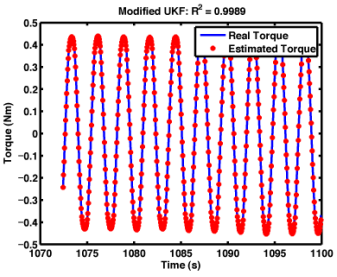

Fig. 8. Real vs Estimated Torque in Yaw: Open Loop Excitation

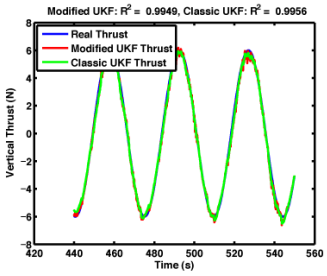

Fig. 9. Real vs Estimated Thrust in Heave: Open Loop Excitation

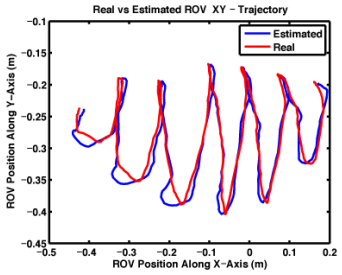

Fig. 10. State Filter: Trajectory in X-Y Plane

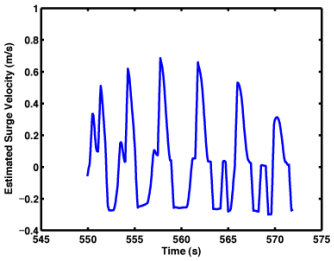

Fig. 11. State Filter: Estimated Surge Velocity

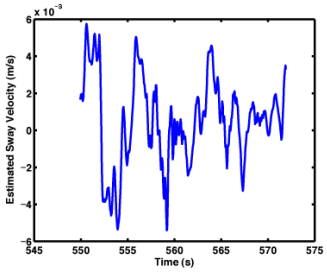

Fig. 12. State Filter: Estimated Sway Velocity

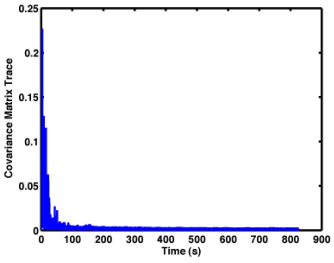

Fig. 13. State Filter: Convergence of Covariance Matrix $\mathbf{P}_{\mathbf{P}_k}$

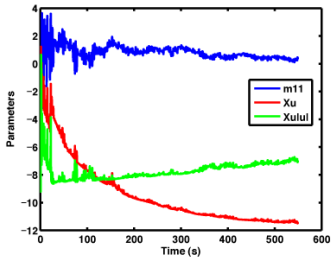

Fig. 14. Parameter Estimation in Surge: Closed Loop Excitation

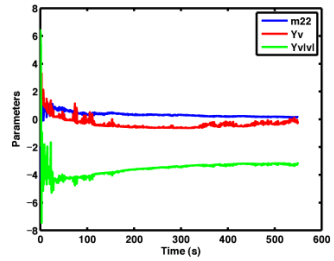

Fig. 15. Parameter Estimation in Sway: Closed Loop Excitation

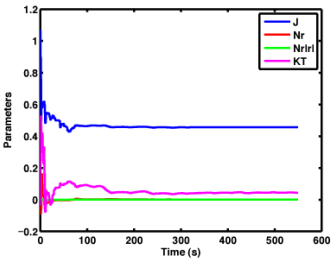

Fig. 16. Parameter Estimation in Yaw: Closed Loop Excitation

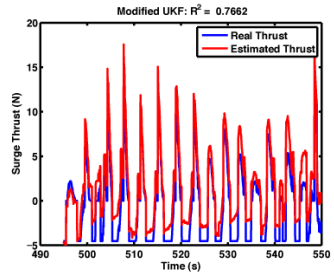

Fig. 17. Real vs Estimated Thrust in Surge: Closed Loop Excitation

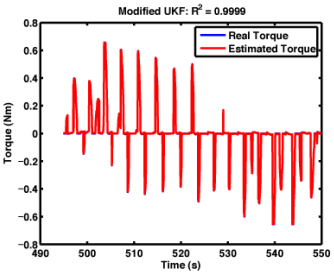

Fig. 18. Real vs Estimated Torque in Yaw: Closed Loop Excitation